PROPERTIES OF UNIAXIAL HEISENBERG ANTIFERROMAGNET BY GREEN FUNCTION METHOD*

By P. Pawlicki, H. Cofta, and Z. Onyszkiewicz

Institute of Physics, A. Mickiewicz University, Poznań**

(Received January 27, 1977)

The collinear two-sublattice antiferromagnet with anisotropic (easy axis) Heisenberg Hamiltonian is investigated for arbitrary spin by means of Green functions in RPA for a wide range of the external magnetic field and temperature. Approximate (within RPA) expressions for the free energy in all phases and for magnetization in the flop phase are derived. The conditions determining the inter-phase boundaries are established. Numerical calculations for the MnF_2 case are carried out giving the full T–H phase diagram from the vanishing of magnetic excitations. Moreover, the following curves are computed: magnetization vs temperature and magnetization vs magnetic field, as well as parallel differential susceptibility vs temperature. Good agreement with the experimental data is achieved.

1. Introduction

The properties of antiferromagnets in a wide range of magnetic field and temperature have commanded the attention of theoreticians for many decades. Let us mention some of the most important steps. The effective field theories have been reviewed exhaustively by Smart [1]. The spin wave treatment was applied by Feder and Pytte [2] to the uniaxial lattice with exchange (two-ion) and one-ion anisotropy. The Green function method in RPA and CD approximations was first used by Anderson and Callen [3] for the case of single-ion anisotropy (but the intermediate phase i. e. the oblique or "flop" phase was not considered in their paper because of the considerable difficulties of decoupling in this region). The "flop" phase has been analyzed using the Green function method by Fu-Cho Pu [4] for the special case of spin 1/2 and isotropic lattice only. Some other less sophisticated method have been used too [5–8]. A review of articles devoted to the magnetic phase diagrams has been given by Shapira and Foner [9].

* Supported by the Institute of Low Temperature and Structure Research, Polish Academy of Sciences, Wrocław.

** Address: Instytut Fizyki, Uniwersytet A. Mickiewicza, Matejki 48/49, 60-769 Poznań, Poland.

In the present work, the Heisenberg model of collinear two-sublattice antiferromagnet with uniaxial anisotropy of exchange interactions is considered. We concentrate our attention on the calculation of the magnetization curves and phase diagram in the plane of T–H parameters. We use the Green function method and apply Tyablikov decoupling for the case of arbitrary spin. An essential feature of this approximaiton is that the spin wave spectrum is temperature-dependent only through the averaged magnetization $\langle \hat{S}_z \rangle$; hence, all calculations have to start from working out this dependence. Since $\langle \hat{S}_z \rangle$ is obtained in implicit form, numerical calculations have to be performed. In order to fix the material parameters before proceeding to the calculation, we have chosen the constants relevant to MnF_2 – one of the best examined antiferromagnets.

2. *The Hamiltonian*

We shall consider the following Hamiltonian with interactions restricted to nearest neighbours only

$$\hat{H} = J \sum_{\alpha<\beta} \hat{\mathbf{S}}(\alpha)\hat{\mathbf{S}}(\beta) + K \sum_{\alpha<\beta} \hat{S}_z(\alpha)\hat{S}_z(\beta) - \mu H \sum_{\alpha} S_z(\alpha) - \mu H \sum_{\beta} S_z(\beta), \tag{1}$$

where μS is the magnetic moment per ion, H – magnetic field in the easy axis direction, J – exchange integral, and K – its anisotropic part, whereas α and β denote sites in the first and second sublattice, respectively. We consider the tetragonal lattice of magnetic ions taking into account only intersublattice interactions. Due to the molecular field calculations of Turov and Irkhin [10], we know the relevant (T, H) quadrant to consist of three regions. For a magnetic field less than a certain critical value $H_1(T)$, we have the antiferromagnetic phase with antiparallel arrangement of spins. In the field H_1, spin flopping takes place; it is a discontinuous transition to the oblique or "flop" phase, in which the spins of the first and second sublattice lie in the same plane parallel to z-direction and form the angles Θ and $-\Theta$, respectively, with the z-axis. At some field $H_2(T)$ (higher than $H_1(T)$ for all temperatures below the triple point, in which H_1 and H_2 coincide) another phase transition occurs, namely a continuous transition to the paramagnetic phase.

To obtain the spin flop transition by the Green function method, one must take into account the oblique phase. To this aim we introduce (following Feder and Pytte [2]) new, local axes of quantization, distinct for both adjacent phases.

2.1. Antiferromagnetic phase

In the expression (1), we perform the substitution

$$\hat{S}_x(\beta) \to \hat{\tilde{S}}_x(\beta), \quad \hat{S}_y(\beta) \to -\hat{\tilde{S}}_y(\beta), \quad \hat{S}_z(\beta) \to -\hat{\tilde{S}}_z(\beta), \tag{2}$$

and, on going over to operators $\hat{S}^+$, $\hat{S}^-$, $\hat{S}_z$, we obtain

$$\hat{H}_a = \tfrac{1}{2} J \sum_{\alpha<\beta} [\hat{S}^+(\alpha)\hat{S}^+(\beta) + \hat{S}^-(\alpha)\hat{S}^-(\beta)]$$

$$-(J+K) \sum_{\alpha<\beta} \hat{S}_z(\alpha)\hat{S}_z(\beta) - \mu H \sum_{\alpha} S_z(\alpha) + \mu H \sum_{\beta} S_z(\beta). \tag{3}$$

2.2. Flop phase

In the expression (1), we carry out the substitution

$$\hat{S}_x(\alpha) \to \hat{\tilde{S}}_x(\alpha),$$

$$\hat{S}_y(\alpha) \to \hat{\tilde{S}}_y(\alpha)\cos\Theta - \hat{\tilde{S}}_z(\alpha)\sin\Theta,$$

$$\hat{S}_z(\alpha) \to \hat{\tilde{S}}_y(\alpha)\sin\Theta + \hat{\tilde{S}}_z(\alpha)\cos\Theta,$$

$$\hat{S}_x(\beta) \to \hat{\tilde{S}}_x(\beta),$$

$$\hat{S}_y(\beta) \to \hat{\tilde{S}}_y(\beta)\cos\Theta + \hat{\tilde{S}}_z(\beta)\sin\Theta,$$

$$\hat{S}_z(\beta) \to -\hat{\tilde{S}}_y(\beta)\sin\Theta + \hat{\tilde{S}}_z(\beta)\cos\Theta, \tag{4}$$

and obtain

$$\hat{H}_f = \tfrac{1}{4}u^2\eta_1 \sum_{\alpha<\beta}[\hat{S}^+(\alpha)\hat{S}^+(\beta)+\hat{S}^-(\alpha)\hat{S}^-(\beta)]$$

$$+\tfrac{1}{4}\eta_2 \sum_{\alpha<\beta}[\hat{S}^+(\alpha)\hat{S}^-(\beta)+\hat{S}^+(\alpha)\hat{S}^+(\beta)]$$

$$+\eta_3 \sum_{\alpha<\beta}\hat{S}_z(\alpha)\hat{S}_z(\beta) - \frac{1}{2i}\mu Hu \sum_{\alpha}[\hat{S}^+(\alpha)-\hat{S}^-(\alpha)]$$

$$+\frac{1}{2i}\mu Hu \sum_{\beta}[\hat{S}^+(\beta)-\hat{S}^-(\beta)] - \mu Hv \sum_{\alpha}\hat{S}_z(\alpha) - \mu Hv \sum_{\beta}\hat{S}_z(\beta), \tag{5}$$

where the following symbols have been used

$$\eta_1 = 2J+K, \quad \eta_2 = (2J+K)\cos^2\Theta - K, \quad \eta_3 = (2J+K)\cos^2\Theta - J,$$

$$u = \sin\Theta, \quad v = \cos\Theta.$$

2.3. Paramagnetic phase

For this phase, no new axes of quantization are needed.

3. The magnetization

3.1. Antiferromagnetic phase

The magnetization of the sublattices is calculated by having recourse to the method introduced by Callen [11]. We define the double-time, retarded Green functions for the α – sublattice as

$$G_{1a} = -i\Theta(t)\langle[\hat{S}^-(\alpha, t), \exp(a\hat{S}_z(\alpha'))\hat{S}^+(\alpha')]\rangle, \tag{6}$$

$$G_{2a} = -i\Theta(t)\langle[\hat{S}^+(\beta, t), \exp(a\hat{S}_z(\alpha'))\hat{S}^+(\alpha')]\rangle, \tag{7}$$

where t denotes time, $\langle\ \rangle$ stands for the canonical average with respect to the density matrix, and a is a parameter. Below, we apply for brevity the notation

$$G_{1a} = \langle\langle \hat{S}^-(\alpha, t)|, \quad G_{2a} = \langle\langle \hat{S}^+(\beta, t)|. \tag{8}$$

On deriving the equations of motion for the functions G_{1a} and G_{2a}, we go over to their Fourier components and apply Tyablikov decoupling. The spectral theorem for Green functions [12] allows us to obtain the following expression for the correlation function

$$\langle \exp(a\hat{S}_z(\alpha))\hat{S}^+(\alpha)\hat{S}^-(\alpha)\rangle$$

$$= \langle [\hat{S}^-(\alpha), \exp(a\hat{S}_z(\alpha))\hat{S}^+(\alpha)]\rangle \frac{1}{N}\sum_k \Phi_a(k), \tag{9}$$

where

$$\Phi_a(k) = \frac{1}{\lambda_{3a}}\left[\frac{\omega_{1a}-\lambda_{1a}}{\exp(\beta\omega_{1a})-1} - \frac{\omega_{2a}-\lambda_{1a}}{\exp(\beta\omega_{2a})-1}\right], \tag{10}$$

$$\omega_{1,2a} = \tfrac{1}{2}[\lambda_{1a}-\lambda_{2a}\pm\lambda_{3a}], \tag{11}$$

$$\lambda_{1a} = \eta_4 z\langle \hat{S}_z(\alpha)\rangle - \mu H, \quad \lambda_{2a} = \eta_4 z\langle \hat{S}_z(\beta)\rangle + \mu H,$$

$$\lambda_{3a} = [\eta_4^2 z^2(\langle \hat{S}_z(\alpha)\rangle + \langle \hat{S}_z(\beta)\rangle)^2 - \eta_5\gamma^2(k)\langle \hat{S}_z(\alpha)\rangle\langle \hat{S}_z(\beta)\rangle]^{1/2},$$

$$\eta_4 = J+K, \quad \eta_5 = 4J^2, \quad \gamma(k) = \sum_\beta \exp(ik\cdot R_{\alpha\beta}). \tag{12}$$

In (12), z denotes the number of nearest neighbours, N – the number of sites of the sublattice, $\sum_k$ – the sum over the first Brillouin zone of the magnetic lattice. By means of the following auxiliary function

$$f(a) = \langle \exp(a\hat{S}_z(\alpha))\rangle, \tag{13}$$

and its derivatives, equation (9) can be written (see Callen [11]) in a form more convenient for further calculations. Callen's method reduces the problem to solving equation (9) with respect to $f(a)$.

We then easily find the equation for magnetization

$$\langle \hat{S}_z(\alpha)\rangle = \frac{\partial f}{\partial a}\bigg|_{a=0} = -\frac{(S-\Phi_a)(1+\Phi_a)^{2S+1}+(S+1+\Phi_a)\Phi_a^{2S+1}}{(1+\Phi_a)^{2S+1}-\Phi_a^{2S+1}}, \tag{14}$$

where

$$\Phi_a = \frac{1}{N}\sum_k \Phi_a(k). \tag{15}$$

The expression for the β-sublattice is similiar and differs from (14) only by the replacement of $\langle \hat{S}_z(\alpha)\rangle$ by $\langle \hat{S}_z(\beta)\rangle$ and by a change in sign of the magnetic field.

3.2 Flop phase

For the flop phase, we define the following Green functions

$$G_{1f} = \langle\langle \hat{S}^-(\alpha, t)|, \quad G_{2f} = \langle\langle \hat{S}^+(\beta, t)|,$$
$$G_{3f} = \langle\langle \hat{S}^-(\beta, t)|, \quad G_{4f} = \langle\langle \hat{S}^+(\alpha, t)|. \tag{16}$$

In order to solve the equations of motion we use, apart of Tyablikov decoupling, the following approximations

$$\langle\langle \hat{S}_z(\alpha)| = 0, \quad \langle\langle \hat{S}_z(\beta)| = 0. \tag{17}$$

In this way we eliminate those functions for which RPA cannot be applied. Next, with the aid of G_{1f}, we obtain the following equation, analogous to (9)

$$\langle \exp(a\hat{S}_z)\hat{S}^+\hat{S}^-\rangle = \langle[\hat{S}^-, \exp(a\hat{S}_z)\hat{S}^+]\rangle \Phi_{1f}$$
$$-(\exp(-a)-1)\langle \exp(a\hat{S}_z)\hat{S}^+\hat{S}^+\rangle \Phi_{2f}, \tag{18}$$

where

$$\Phi_{1f} = \frac{1}{N}\sum_k \left[\frac{\lambda_{1f}-\lambda_{2f}}{4\omega_{1f}} \operatorname{cth}(\tfrac{1}{2}\beta\omega_{1f}) + \frac{\lambda_{1f}+\lambda_{2f}}{4\omega_{2f}} \operatorname{cth}(\tfrac{1}{2}\beta\omega_{2f})\right] - \tfrac{1}{2}, \tag{19}$$

$$\Phi_{2f} = \frac{1}{N}\sum_k \left[\frac{\lambda_{3f}}{4\omega_{1f}} \operatorname{cth}(\tfrac{1}{2}\beta\omega_{1f}) - \frac{\lambda_{3f}}{4\omega_{2f}} \operatorname{cth}(\tfrac{1}{2}\beta\omega_{2f})\right], \tag{20}$$

$$\omega_{1,2f} = [(\lambda_{1f} \mp \lambda_{2f})^2 - \lambda_{3f}^2]^{1/2}, \tag{21}$$

$$\lambda_{1f} = \langle \hat{S}_z(\alpha)\rangle z\eta_3 - \mu H v, \quad \lambda_{2f} = \tfrac{1}{2}\langle \hat{S}_z(\alpha)\rangle \eta_2 \gamma(\boldsymbol{k}),$$
$$\lambda_{3f} = \tfrac{1}{2}u^2\eta_1\langle \hat{S}_z(\alpha)\rangle \gamma(\boldsymbol{k}).$$

It is not possible to write the last average in Eq. (18) in terms of the function (13), as in the antiferromagnetic case. Therefore, we propose here another way of solving the problem; namely, with the aid of the functioh G_{4f}, we obtain

$$\langle \exp(a\hat{S}_z)\hat{S}^+\hat{S}^+\rangle = \langle[\hat{S}^-, \exp(a\hat{S}_z)\hat{S}^+]\rangle \frac{\Phi_{2f}}{1+[\exp(-a)-1](\Phi_{1f}+\frac{1}{2})}. \tag{22}$$

We can now eliminate the term $\langle \exp(a\hat{S}_z)\,\hat{S}^+\hat{S}^+\rangle$ from Eqs. (18) and (22); this leads to the following differential equation

$$f''(a) - f'(a)\frac{[(\Phi_{1f}+1)^2-\Phi_{2f}^2]e^{-a} - (\Phi_{1f}^2-\Phi_{2f}^2)e^a}{[(\Phi_{1f}+1)^2-\Phi_{2f}^2]e^{-a} + (\Phi_{1f}^2-\Phi_{2f}^2)e^a - 2(\Phi_{1f}^2+\Phi_{1f}-\Phi_{2f}^2)}$$
$$-S(S+1)f(a) = 0. \tag{23}$$

Using the boundary conditions [11], we thus find the solution of Eq. (23) and obtain expressions for the magnetization, for each value of the spin separately[1].
The resulting implicit equation has the following form

$$\langle S_z\rangle = -\frac{(S-\Phi_{1f})(1+\Phi_{1f})^{2S+1}+(S+1+\Phi_{1f})\Phi_{1f}^{2S+1}+\chi_S}{(1+\Phi_{1f})^{2S+1}-\Phi_{1f}^{2S+1}+\xi_S} \tag{24}$$

where χ_S and ξ_S are given in Table I for spin $S = 1/2 \ldots 5/2$. Above, we have put

$$\langle \hat{S}_z(\alpha)\rangle = \langle \hat{S}_z(\beta)\rangle = \langle \hat{S}_z\rangle, \tag{25}$$

TABLE I

Formulae of the symbols χ_S, ξ_S

S	χ_S	ξ_S
$\frac{1}{2}$	0	0
1	0	Φ_{2f}^2
$\frac{3}{2}$	$\frac{5}{2}\Phi_{2f}^2$	$2\Phi_{2f}^2(2\Phi_{1f}+1)$
2	$7\Phi_{2f}^2(2\Phi_{1f}+1)$	$\Phi_{2f}^4+\Phi_{2f}^2(10\Phi_{1f}^2+10\Phi_{1f}+\frac{11}{3})$
$\frac{5}{2}$	$\frac{35}{6}\Phi_{2f}^4+\Phi_{2f}^2(\frac{140}{3}\Phi_{1f}^2$ $+\frac{140}{3}\Phi_{1f}+\frac{231}{16})$	$3\Phi_{2f}^4(2\Phi_{1f}+1)+\Phi_{2f}^2(20\Phi_{1f}^3$ $+30\Phi_{1f}^2+\frac{87}{4}\Phi_{1f}+\frac{47}{8})$

Note that $\chi_{1/2}$ and $\xi_{1/2}$ are equal to zero because $\langle \exp(a\hat{S}_z)\hat{S}^+\hat{S}^+\rangle$ of Eq. (22) vanishes in this case as follows from the operator identity $\hat{S}^+\hat{S}^+ = 0$ for $S = 1/2$.

in conformity with the symmetry of the Hamiltonian.

At angle $\Theta = 0$, Eq. (24) obviously reduces to that obtained within RPA for the paramagnetic phase, implying $\Phi_{2f} = 0$. The condition for the angle Θ can be obtained by minimalization of the free energy (for a discussion, see Section 6).

---

[1] Our solution is found in the form of a series

$$f(a) = \sum_{\nu=0}^{\infty} b_\nu a^\nu.$$

The coefficients are given by a set of simultaneous equations as

$$b_\nu = b_\nu(b_{\nu-1}, b_{\nu-2}, \ldots b_0).$$

Therefore, the expansion has to be carried out step by step. Moreover, the boundary condition [11]

$$\prod_{p=-S}^{S}(\hat{S}_z - p) = 0$$

must be considered for each value of the spin separately. This complicates the calculations so much that we give here the final result only.

3.3. Paramagnetic phase

The magnetization in the paramagnetic region can be expressed by equation (24) with $\Theta = 0$. We obtain

$$\chi_S, \quad \xi_S \to 0, \quad \Phi_a \to \Phi_p = \frac{1}{2N} \sum_k \frac{1}{\exp(\beta\omega_p) - 1}, \tag{26}$$

where

$$\omega_p = (J+K)z\langle \hat{S}_z \rangle - J\langle \hat{S}_z \rangle \gamma(\boldsymbol{k}) - \mu H. \tag{27}$$

4. The free energy

With the aim of calculating the free energy, it is convenient to introduce a formal parameter g into the Hamiltonian, writing

$$\hat{H} = \hat{H}_0 + g\hat{H}_1, \tag{28}$$

where $\hat{H}_0$ includes only the terms for which the sum of states can be computed explicitly (terms of the Zeeman type). In this case, the free energy per ion can be expressed as follows:

$$F = F_0 + F_1 = -\frac{1}{\beta} \ln \operatorname{Tr} \exp(-\beta\hat{H}_0) + \int_0^1 \langle \hat{H}_1 \rangle dg. \tag{29}$$

The average $\langle \hat{H}_1 \rangle$ is computed applying the Green function method to the Hamiltonian (28) including the parameter g. Following Waks et al. [13], we write fully the Ising type terms occuring in the Hamiltonian with the aim to separate the terms of Zeeman type from those describing the fluctuations

$$\sum_{\alpha<\beta} \hat{S}_z(\alpha)\hat{S}_z(\beta) = -Nz\langle \hat{S}_z(\alpha) \rangle \langle \hat{S}_z(\beta) \rangle + \langle \hat{S}_z(\alpha) \rangle \sum_\beta \hat{S}_z(\beta)$$

$$+ \langle \hat{S}_z(\beta) \rangle \sum_\alpha \hat{S}_z(\alpha) + \sum_{\alpha<\beta} [\hat{S}_z(\alpha) - \langle \hat{S}_z(\alpha) \rangle] [\hat{S}_z(\beta) - \langle \hat{S}_z(\beta) \rangle]. \tag{30}$$

The omission of fluctuations of the spin z-components is consistent with RPA and allows us to include the Ising type terms into the F_0 part of the free energy. The correlation functions for nearest neighbours used for computing the free energy are listed in Table II. The expressions for the free energy are given below.

TABLE II

List of the correlation functions used to compute the free energy (α, β denote nearest neighbours)

Antiferromagnetic phase

$$\langle \hat{S}^-(\alpha)\hat{S}^-(\beta)\rangle = \frac{1}{N}\sum_k \left[\frac{1}{1-\exp(-\beta\omega_{1a})} - \frac{1}{1-\exp(-\beta\omega_{2a})}\right]\frac{\mu_a}{\lambda_{3a}} e^{ik\cdot R_{\alpha\beta}}$$

$$\mu_a = -2\langle \hat{S}_z(\alpha)\rangle \langle \hat{S}_z(\beta)\rangle J\gamma(k),$$

$$\langle \hat{S}^+(\alpha)\hat{S}^+(\beta)\rangle_\omega = -\langle \hat{S}^-(\alpha)\hat{S}^-(\beta)\rangle_{-\omega}.$$

Flop phase

$$\langle \hat{S}^+(\alpha)\hat{S}^+(\beta)\rangle = -\frac{\langle \hat{S}_z\rangle}{N}\sum_k \left[\frac{\lambda_{3f}}{\omega_{1f}}\operatorname{cth}(\tfrac{1}{2}\beta\omega_{1f})\right] e^{ik\cdot R_{\alpha\beta}},$$

$$\langle \hat{S}^-(\alpha)\hat{S}^-(\beta)\rangle = \langle \hat{S}^+(\alpha)\hat{S}^+(\beta)\rangle,$$

$$\langle \hat{S}^+(\alpha)\hat{S}^-(\beta)\rangle = -\frac{\langle \hat{S}_z\rangle}{N}\sum_k \left[\frac{\lambda_{1f}-\lambda_{2f}}{\omega_{1f}}\operatorname{cth}(\tfrac{1}{2}\beta\omega_{1f})\right] e^{ik\cdot R_{\alpha\beta}},$$

$$\langle \hat{S}^-(\alpha)\hat{S}^+(\beta)\rangle = \langle \hat{S}^+(\alpha)\hat{S}^-(\beta)\rangle.$$

Paramagnetic phase

$$\langle \hat{S}^-(\alpha)\hat{S}^+(\beta)\rangle = -\frac{\langle \hat{S}_z\rangle}{N}\sum_k \frac{1}{1-\exp(-\beta\omega_p)} e^{ik\cdot R_{\alpha\beta}},$$

$$\langle \hat{S}^+(\alpha)\hat{S}^-(\beta)\rangle_\omega = -\langle \hat{S}^-(\alpha)\hat{S}^+(\beta)\rangle_{-\omega}.$$

4.1. Antiferromagnetic phase

$$F_{0a} = -\frac{1}{2\beta}\left[\ln\frac{\sinh(\beta\lambda_{2a}(S+\frac{1}{2}))}{\sinh(\beta\lambda_{2a}\frac{1}{2})} + \ln\frac{\sinh(\beta\lambda_{1a}(S+\frac{1}{2}))}{\sinh(\beta\lambda_{1a}\frac{1}{2})}\right] + \tfrac{1}{2}z\eta_4\langle \hat{S}_z(\alpha)\rangle\langle \hat{S}_z(\beta)\rangle, \quad (31)$$

$$F_{1a} = \frac{1}{2N\beta}\sum_k [\ln(1-\exp(-\beta\omega_{1a})) + \ln(1-\exp(\beta\omega_{2a})) - \ln(1-\exp(\beta\lambda_{1a}))$$

$$-\ln(1-\exp(\beta\lambda_{2a}))] + \frac{1}{4N}\sum_k (\lambda_{1a}+\lambda_{2a}+\lambda_{3a}). \quad (32)$$

4.2. Flop phase

$$F_{0f} = -\frac{1}{\beta}\ln\frac{\sinh(\beta\lambda_{1f}(S+\frac{1}{2}))}{\sinh(\beta\lambda_{1f}\frac{1}{2})} - \tfrac{1}{2}\eta_3 z\langle\hat{S}_z\rangle^2, \tag{33}$$

$$F_{1f} = \frac{1}{2N\beta}\sum_k [\ln(1-\exp(-\beta\omega_{1f}))+\ln(1-\exp(-\beta\omega_{2f}))$$

$$-2\ln(1-\exp(-\beta\lambda_{1f}))] + \frac{1}{4N}\sum_k(\omega_{1f}+\omega_{2f}-2\lambda_{1f}). \tag{34}$$

4.3. Paramagnetic phase

$$F_{0f} = -\frac{1}{\beta}\ln\frac{\sinh(\beta\lambda_p(S+\frac{1}{2}))}{\sinh(\beta\lambda_p\frac{1}{2})} - \tfrac{1}{2}z\langle\hat{S}_z\rangle^2\eta_4, \tag{35}$$

$$F_{1p} = \frac{1}{2N\beta}\sum_k [\ln(1-\exp(-\beta\omega_p))-\ln(1-\exp(-\beta\lambda_p))], \tag{36}$$

where

$$\lambda_p = -\mu H+\eta_4 z\langle\hat{S}_z\rangle.$$

It is necessary to point out that, when computing the free energy form equation (29), we have neglected the implicit dependence of the averaged magnetization on the parameter g. Therefore, this can be seen as a first step of iteration. But even in this case the expressions for the averaged hamiltonian are rather complicated.

5. *The antiferromagnetic — flop phase boundary*

The boundaries of existence separating the antiferromagnetic and flop phases in the T-H plane can be obtained from the vanishing of magnetic excitation energy i. e. from the poles of the Green functions. In the antiferromagnetic phase, the energy minimum of the lower spin wave branch (ω_{2a} from Eq. (10) occurs for magnons with $k = [0, 0, 0]$. Thus the condition

$$\omega_{2a}(\boldsymbol{k} = [0, 0, 0]) = 0 \tag{37}$$

determines the temperature dependence of the critical magnetic field. For $T = 0$, this condition yields the well known formula

$$\mu H_{1a} = z\langle\hat{S}_z\rangle(K(2J+K))^{1/2}. \tag{38}$$

Starting from the flop phase, or using the equilibrium condition

$$F_{0f} = F_{0a}, \tag{39}$$

we obtain te same expression (38). This means that these three conditions give the same value for the critical field when zero point spin deviations are ignored. The magnitude of the latter can easily be estimated from the low temperature expansion of magnetization. We obtain for the b. c. c lattice the following expansion of equation (38).

$$H_{1a} = H_1^0\left(1+\frac{1}{2S}\delta_0+\frac{1}{2S}\delta_T\right), \tag{40}$$

where

$$\delta_0 = -\frac{1}{N}\sum_k \frac{1+\tilde{K}}{[(1+\tilde{K})^2-\gamma^2(k)/z^2]^{1/2}}+1,$$

$$\delta_T = -\frac{2^{3/2}}{\pi^2}[(1+\tilde{K})\tilde{K}(1+\tfrac{1}{2}\tilde{K})-\tfrac{1}{2}\tilde{K}^{3/2}(2+\tilde{K})^{3/2}]$$

$$\times\left(\frac{1}{\beta\mu H_1^0}\right)^{3/2}\Gamma(\tfrac{3}{2})\zeta(\tfrac{3}{2})+\frac{2^{2/3}}{\pi^2}(1+\tilde{K})\tilde{K}(1+\tfrac{1}{2}\tilde{K})\left(\frac{1}{\beta\mu H_1^0}\right)^{5/2}\Gamma(\tfrac{5}{2})\zeta(\tfrac{5}{2})+\ldots,$$

$$\mu H_1^0 = zS[K(2J+K)]^{1/2}, \quad \tilde{K} = K/J.$$

From the flop-phase side we obtain

$$H_{1f} = H_1^0\left(1+\frac{1}{2S}\delta_0+\frac{1}{2S}\delta_T\right), \tag{41}$$

where

$$\delta_0 = 1-\frac{1}{N}\sum_k \frac{1}{(1-\gamma^2(k)/z^2)^{1/2}},$$

$$\delta_T = -\frac{8}{\pi^2}\left(\frac{1}{\beta JzS}\right)^2\Gamma(2)\zeta(2)+\ldots.$$

These equations are identical with those obtained by Feder and Pytte [2] applying the spin wave method except for the term $T^{3/2}$, which is absent in the spin wave treatment. From expressions (40) and (41) hysteresis is seen to vanish with increasing temperature if $\tilde{K}^{1/2} \ll 1$ only, as follows from the spurious term $T^{3/2}$.

In the example we consider below, $\tilde{K} = 0.01$ and hysteresis for zero temperature is of the order of 2%. Consequently, the condition (38) determines with good accuracy the phase boundary between the antiferromagnetic and the flop phase.

6. Boundary between the paramagnetic and two other phases

In order to determine the boundary of existence of the paramagnetic phase, we use the method described in Section 5 (at decreasing magnetic field). The condition now reads

$$\omega_p\left(\boldsymbol{k} = \left[\frac{\pi}{a}, \frac{\pi}{a}, \frac{\pi}{c}\right]\right) = 0 \tag{42}$$

and yields

$$\mu H_2 = z\langle \hat{S}_z \rangle (2J+K). \tag{43}$$

When starting from the flop phase, one needs an additional equation for the angle Θ. We adopt here the molecular field condition

$$\frac{\partial F_0}{\partial \Theta} = 0, \tag{44}$$

which gives

$$\cos \Theta = \frac{\mu H}{z(2J+K)\langle \hat{S}_z \rangle}. \tag{45}$$

We believe this expression to be correct in RPA also because, when using it, the modes of the flop phase soften along the same $H(T)$-curve as given by equation (43), as expected for a continuous phase transition.

On the boundary separating the antiferro- and paramagnetic phases, some difficulties occur because the condition (43) does not coincide with the behaviour of the magnetization $M(H, T)$. Namely, considering the equations for magnetization for low magnetic fields, we obtain for the boundary between these two phases

$$\mu H = z\langle \hat{S}_z \rangle (2J+2K), \tag{46}$$

what yields for b. c. c. lattice the Néel temperature

$$k_B T_N = \tfrac{1}{3} S(S+1) z J I^{-1}[(1+\tilde{K})^{-1}], \tag{47}$$

whereas equation (43) gives the lower value

$$k_B T_N = \tfrac{1}{3} S(S+1) z I^{-1}(1), \tag{48}$$

where I is a Watson integral [16]. The antiferromagnetic modes soften between the curves (43) and (46). These differences arise because in RPA the anisotropy K is independent of the wave vector (meaning that it is treated as in MFA, contrary to the exchange integral). In our numerical calculations, we use the condition (43).

7. Application to MnF_2

Manganese fluoride has a rutile type structure with two Mn^{++} ions ($S = 5/2$) in the unit cell. Each spin in the central site is ferromagnetically coupled along the tetragonal axis with its two nearest neighbours lying at the centres of adjacent cells and strongly

coupled by antiferromagnetic interactions with its eight next nearest neighbours, localized in the corners of the same unit cell. Following Smart [1], we neglect the n. n. coupling because it is thirty times weaker than the n. n. n. coupling. To carry out the numerical calculations, well specified values of the exchange integral I and anisotropy K are obviously needed. We evaluate them from Eq. (48) for T_N and Eq. (38) for the threshold field $H_1(T = 0)$ adopting here the following experimental data: $H_1 = 96$ kOe [14] and $T_N = 67.34$ K [9], which yield $I/k_B = 2.01$ K and $K/k_B = 0.02$ K. For these values, we

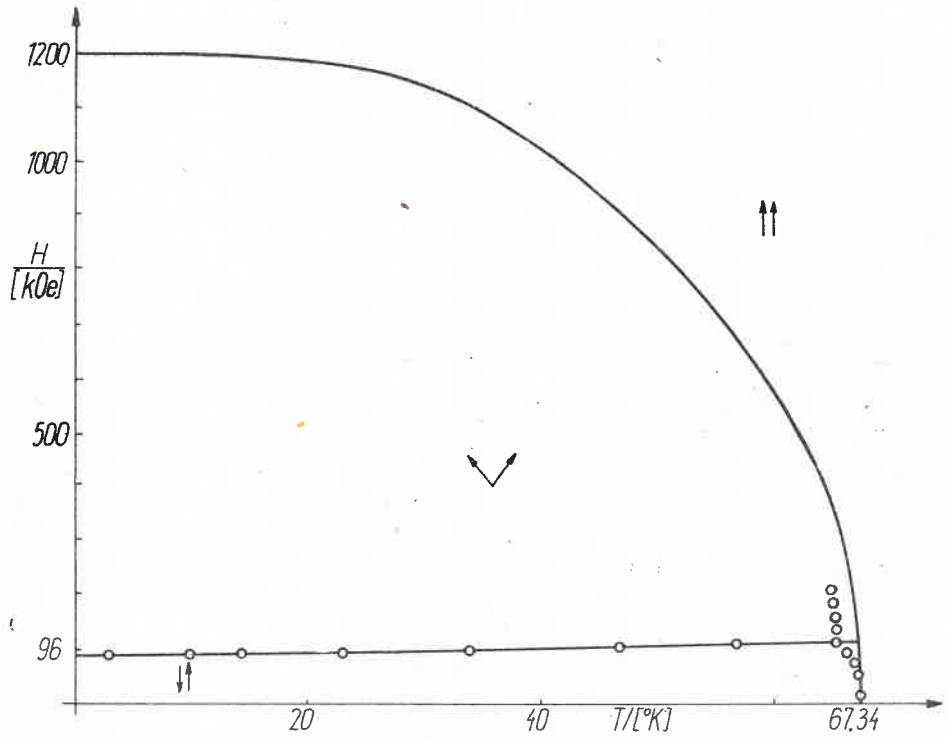

Fig. 1. Phase boundaries in the T–H plane. Circles denote experimental values of Shapira and Foner [9]

computed the phase diagram (Fig. 1). To facilitate comparison with experiment, we show in the same diagram the results of measurements by Shapira and Foner [9]. Good agreement with our theoretical results is found except in the vicinity of the triple point. This discrepancy is caused by our use of the same condition (43) for both boundaries, corresponding to para-flop and para-antiferromagnetic transitions.

The hysteresis of the first-order (flop to antiferro) phase transition is, in fact, negligibly small. We obtain for zero temperature

$$H_{1a} = 0.978 H_0, \tag{49}$$

$$H_{1f} = 0.976 H_0, \tag{50}$$

and this difference vanishes with increasing temperature as shown in Section 5.

Before computing the phase diagram, it was necessary to obtain the magnetization vs temperature and magnetization vs magnetic field curves. Some of these curves are shown in Figs 2 and 3. Fig. 2 shows the temperature dependence of sublattice magnetization for $H = 50$ kOe in the phase diagram as obtained by numerical solution of the equations of Section 3.1 and 3.3. We note that sublattice magnetization does not attain its saturation

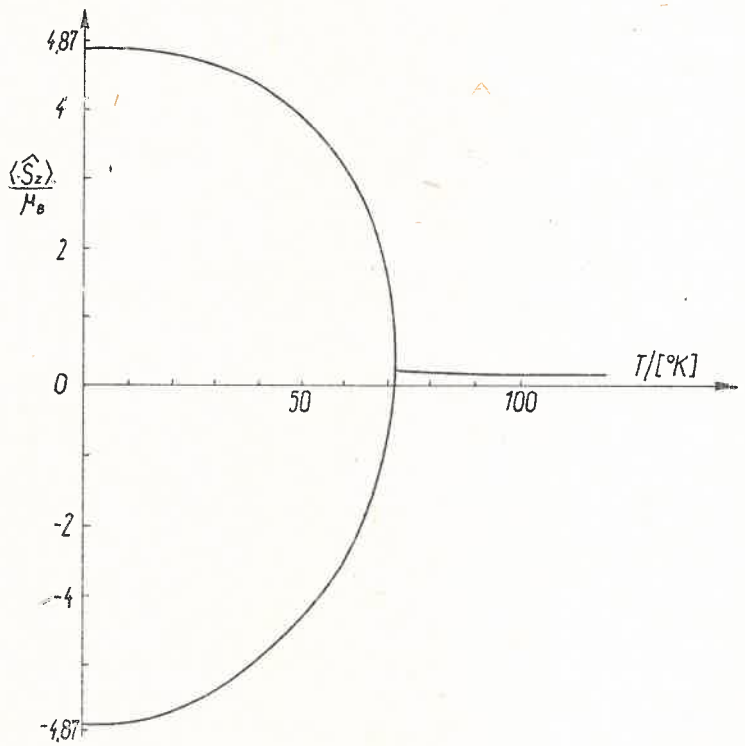

Fig. 2. Sublattice magnteization vs temperature for magnetic field $H = 50$ kOe parallel to the antiferromagnetic direction

value because of the zero-point spin deviation (independent of the magnetic field). The Néel temperature predicted by formula (14) is 72 K (which differs by 7% from that obtained from the phase diagram). The magnetization curve taken along the line $H = 1500$ kOe (paramagnetic region) is shown in Figure 3. The long paramagnetic tail is caused by the strong magnetic field. Figure 4 shows the computed magnetic field dependence of macroscopic magnetization M at various temperatures. In the antiferromagnetic phase we have

$$M = \tfrac{1}{2}(\langle \hat{S}_z(\alpha) \rangle - \langle \hat{S}_z(\beta) \rangle). \tag{51}$$

Comparison with measurements by Gunzbourg and Krebs [15] shows substantial differences We presume that their experimental magnetization curves lie too high, with a slope

attaining its maximal value for $T = 60$ K, and it is not clear what will happen at higher temperatures. In the flop phase.

$$M = \langle \hat{S}_z \rangle \cos \Theta \text{ (note Eq. (25))}, \tag{52}$$

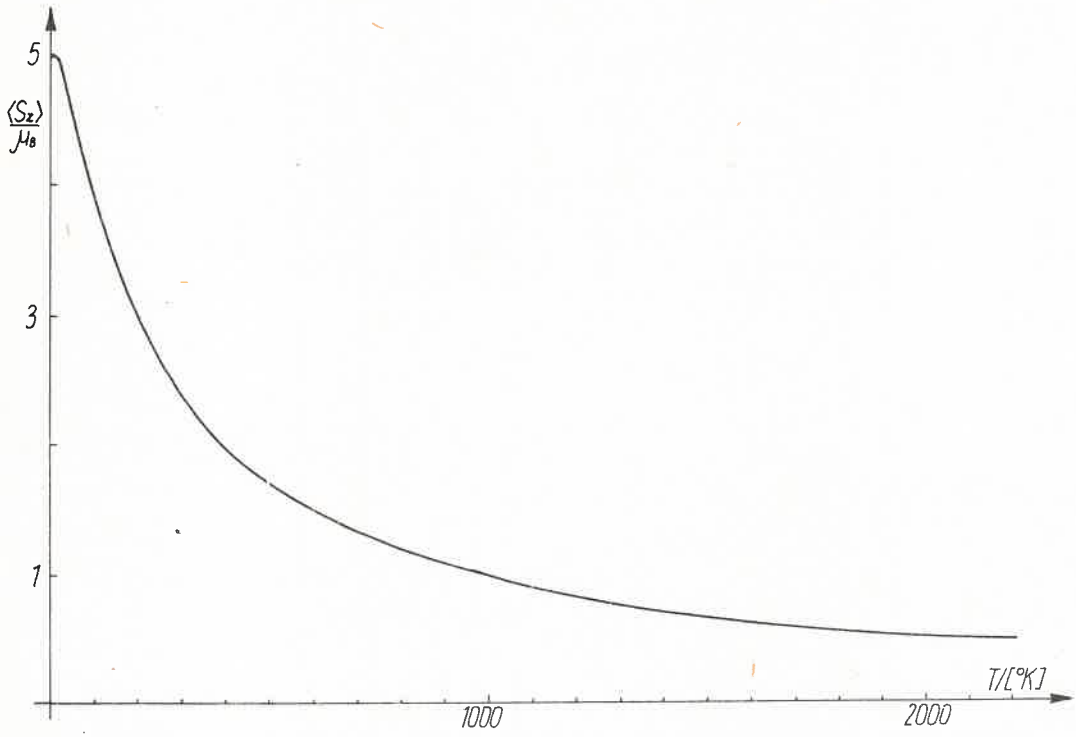

Fig. 3. Magnetization vs temperature for magnetic field $H = 1400$ kOe parallel to antiferromagnetic direction. (Paramagnetic phase)

where $\cos \Theta$ is given by Eq. (45). Thus,

$$M = \frac{\mu H}{z(2J+K)} \tag{53}$$

and we conclude that the macroscopic magnetization is independent of temperature, as has been confirmed experimentally [15].

Knowledge of the magnetization curves permits the numerical computation of the parallel differential susceptibility. Its temperature dependence for various fields is shown in Fig. 5 as obtained by numerical differentiation of the magnetization curves (except for the flop phase, for which the result was obtained directly from Eq. (53)). Good agreement with the measurements for the antiferromagnetic phase ($H = 0$) is obvious. For high magnetic fields, the susceptibility has a strongly broadened maximum. Similar results are obtained for the specific heat vs temperature suggesting that the paramagnetic region actually decays into two subregions separated by a broadened transition line.

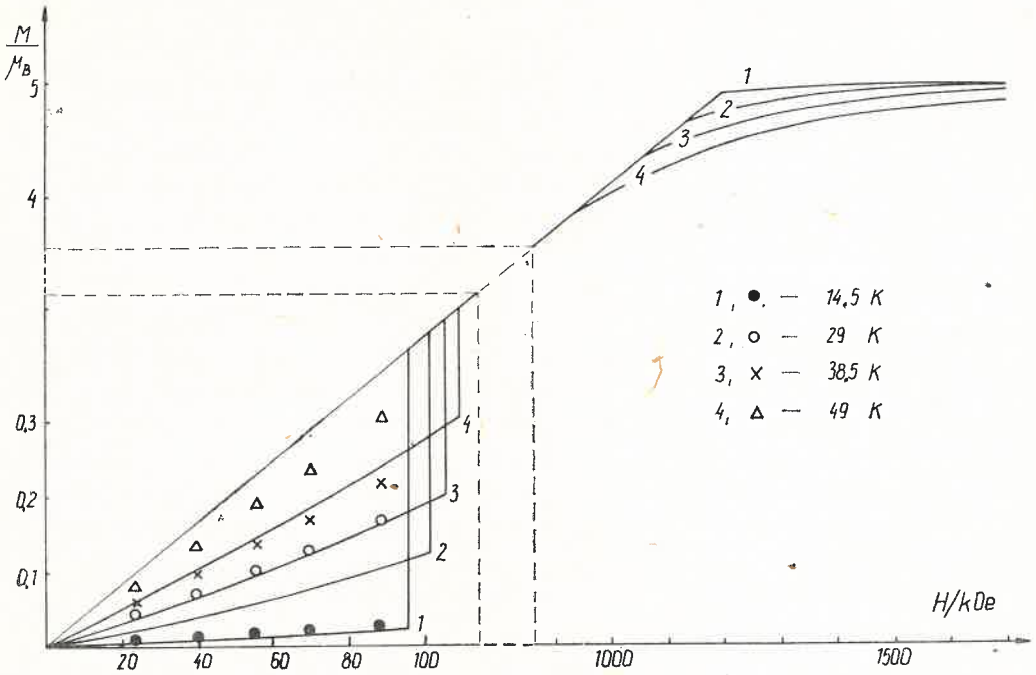

Fig. 4. Magnetization vs magnetic field for various temperatures. Points ● ○ × ▲ denotes experimental values from measurements by Gunzbourg and Krebs [15]

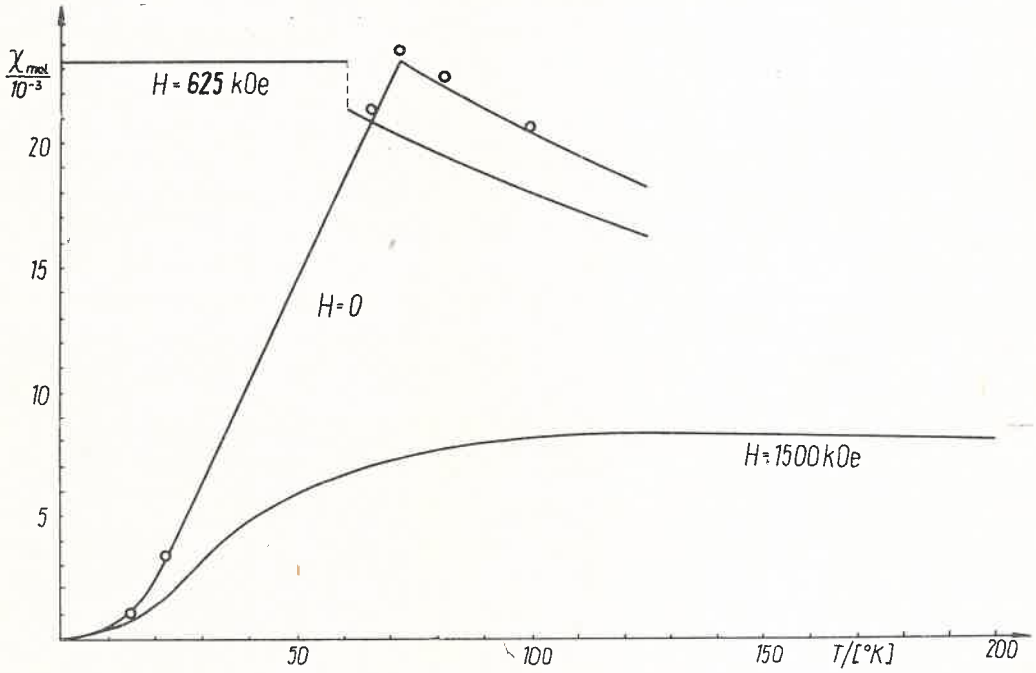

Fig. 5. Parallel susceptibility vs temperature for various magnetic field. Circles denote experimental values from the work of Bizette and Tsai [17]

8. Conclusions

To investigate theoretically the behaviour of a typical collinear antiferromagnet in the whole range of thermodynamic variables H and T, one must use a method ensuring good approximation for all temperatures. The Green functions in the Random Phase Approximation, when used here, turned out to be an appropriate tool for our purpose. To obtain the full phase diagram, we took into consideration the flop phase, disregarded by some authors (Eq. [3]) because of the great difficulties of decoupling in this region. For this reason some further approximations are used in this paper (see Sec. 3.2) in order to derive the magnetization formula.

Contrary to Ref. [4], our approach is valid for arbitrary spin and takes into account magnetic anisotropy (of the two-ion type). The phase diagram thus obtained (Fig. 1) shows excellent agreement with experiment on the antiferro-flop transition line. On this line (which is of first order in Ehrenfest classification) only a negligibly small hysteresis caused by the zero point spin deviation is obtained as in spin wave theory [2]. Nevertheless it can be easily shown that taking into account next nearest neighbours as well as the one-ion anisotropy allows us to obtain greater hysteresis. On the second-order transition line some difficulties arise:

— the Néel temperature cannot be determined unambiguously, as was first shown by Anderson and Callen [3], and

— no discontinuity in the slope of the boundary line in the triple point was obtained due to our use of the same condition for the para-flop and para-antiferromagnetic transition line. Obviously, the high field regions of our phase diagram are not accessible to experiment in the case of MnF_2 making our comparison less complete.

The magnetization curves obtained here are of the typical shape. Especially in flop phase we get a very simple expression (53) analogous to that resulting from MFA. This simplicity leads to a constant susceptibility in the whole flop phase (Fig. 5) strictly equal to the maximum of the susceptibility curve for $H = 0$. This last curve exhibits excellent agreement with experiment especially in the low temperature region.

It is worth noting that we have achieved satisfactory agreement with the experimental results notwithstanding the fact that we replaced here the one-ion anisotropy (which can play an important role in the case of MnF_2) by anisotropy of the Heisenberg Hamiltonian because of its mathematical simplicity.

The authors wish to thank Dr. R. Micnas for his helpful discussions.

REFERENCES

[1] J. S. Smart, *Effective Field Theories of Magnetism*, Philadelphia–London 1966.
[2] J. Feder, E. Pytte, *Phys. Rev.* **168**, 640 (1968).
[3] F. B. Anderson, H. B. Callen, *Phys. Rev.* **136**, 1068 (1964).
[4] Fu-Cho Pu, *Dokl. Akademii Nauk SSSR* **131**, 1244 (1960).
[5] H. Falk, *Phys. Rev.* **135A**, 1382 (1964).
[6] M. A. Savchenko, B. B. Tarasenko, *Fiz. Tver. Tela* **9**, 3284 (1967).
[7] B. R. Morrison, *Phys. Status Solidi* (b) **59**, 581 (1973).

[8] N. Yamashita, *J. Phys. Soc. Jap.* **32**, 610 (1972).
[9] Y. Shapira, S. Foner, *Phys. Rev.* **18**, 3083 (1970).
[10] E. A. Turov, I. P. Irkhin, *Izv. Akad. Nauk SSSR* **22**, 1168 (1958).
[11] H. B. Callen, *Phys. Rev.* **130**, 890 (1963).
[12] D. V. Zubarev, *Usp. Fiz. Nauk*, 71 (1960).
[13] V. G. Vaks, A. I. Larkin, *Zh. Eksper. Teor. Fiz.* **53**, 211 (1967).
[14] I. S. Jacobs, *J. Appl. Phys.* **32***S*, 61 (1961).
[15] I. de Gunzbourg, J. P. Krebs, *J. Phys. (France)* **29**, 42 (1968).
[16] I. Mannari, C. Kawabata, Research Notes of Dep. Phys. Okayama University, Japan 1964.
[17] H. Bizette, B. Tsai, *Compt. Rend.* **238**, 1575 (1954).